agronomy

MDPI

Article

Integrative Transcriptomic and Metabolomic Analysis Reveals the Molecular Mechanisms Underlying Flowering Time Variation in *Camellia* Species

Ling Zhou [1,2,†], Tao Guo [1,2,†], Shihui Zou [1,2], Lingli Li [1,2], Xuemei Li [1,2], Jiao Wang [1,2], Zilin Zhu [1,2] and Lijiao Ai [1,2,*]

[1] Chongqing Key Laboratory of Germplasm Innovation and Utilization of Native Plants, Chongqing Landscape and Gardening Research Institute, Chongqing 401329, China; zhoulingym@163.com (L.Z.); yushen0002008@126.com (T.G.); zoushihui861020@126.com (S.Z.); linglil009@163.com (L.L.); lxmzoe@163.com (X.L.); sudamasaki0708@163.com (J.W.); zzl126126126@126.com (Z.Z.)
[2] Chongqing Urban Landscaping Engineering Technology Research Center, Chongqing Landscape and Gardening Research Institute, Chongqing 401329, China
* Correspondence: alj01461@foxmail.com
† These authors contributed equally to this work.

Abstract: *Camellia*'s ornamental value is constrained by its natural winter–spring flowering period. Although the discovery of *Camellia azalea* provides important germplasm resources for developing cultivars with year-round flowering, the molecular mechanisms underlying flowering time variation remain unclear. Here, we investigated three germplasms with distinct flowering patterns: winter–spring flowering *Camellia japonica* 'Tieke Baozhu', summer–autumn flowering *Camellia azalea*, and their hybrid *Camellia* 'Lingnan Yuanbao' inheriting the latter's flowering traits. Integrated transcriptomic and metabolomic analyses revealed that differentially expressed genes (DEGs) and metabolites (DAMs) were mainly enriched in the pathways related to photoperiod regulation, plant hormone synthesis and signal transduction and flavonoid synthesis. The transcription factor (TF) analysis revealed that the bHLH and MYB TF families were significantly differentially expressed in different *Camellia* germplasm, suggesting their potential involvement in the regulation of flowering time through the plant hormone signal transduction and photoperiod pathway. Meanwhile, photoperiod regulation related genes, including Cryptochrome circadian regulator (*CRY*), Timing of CAB expression 1 (*TOC1*), and phytochrome interacting factor 3 (*PIF3*), showed significant expression differences, further confirming the photoperiod pathway's crucial regulatory function. In terms of plant hormone levels, there were significant differences in the levels of gibberellin (GA), abscisic acid (ABA), and jasmonic acid (JA) among *Camellia* germplasm. The differential expression characteristics of DELLA (Asp-Glu-Leu-Leu-Ala) proteins indicated that the GA signal transduction pathway was one of the key factors regulating flowering time in *Camellia*. Additionally, metabolomics analyses showed significant differences in flavonoid metabolite content among *Camellia* germplasm, which was significantly correlated with the different developmental stages of the buds. Our findings provide a theoretical basis for the molecular breeding of everblooming *Camellia* cultivars, advancing the understanding of flowering regulation mechanism in ornamental species.

Keywords: *Camellia*; transcriptome; metabolome; flowering time; photoperiod; plant hormones; flavonoids

check for updates

Received: 26 March 2025
Revised: 29 April 2025
Accepted: 6 May 2025
Published: 24 May 2025

Citation: Zhou, L.; Guo, T.; Zou, S.; Li, L.; Li, X.; Wang, J.; Zhu, Z.; Ai, L. Integrative Transcriptomic and Metabolomic Analysis Reveals the Molecular Mechanisms Underlying Flowering Time Variation in *Camellia* Species. *Agronomy* **2025**, *15*, 1288. https://doi.org/10.3390/agronomy15061288

Copyright: © 2025 by the authors. Licensee MDPI, Basel, Switzerland. This article is an open access article distributed under the terms and conditions of the Creative Commons Attribution (CC BY) license (https://creativecommons.org/licenses/by/4.0/).

1. Introduction

Camellia japonica, a woody shrub or small arbor from the Theaceae family [1,2], boasts an elegant plant structure, lush evergreen leaves, and vibrant blossoms, making it a highly promising choice for diverse landscaping applications [3]. As an important ornamental genus, *Camellia* species are widely cherished worldwide for their cultural symbolism and economic value [4]. However, most cultivars, including *C. japonica*, concentrate flowering in late winter to early spring [5,6], which limits their ornamental utility and market competitiveness. This constraint highlights the urgent need to develop cultivars with year-round flowering through molecular breeding strategies. *Camellia azalea* is native to Yangchun County, Guangdong Province, China, which uniquely blooms from June to October [6]. The discovery of *C. azalea* has provided possibilities for extending the flowering time. This species has been used as a paternal parent in hybridization programs, with its hybrid progeny *Camellia* 'Lingnan Yuanbao' (derived from crossing *C. japonica* 'Tieke Baozhu' and *C. azalea*) demonstrating summer flowering characteristics.

As an important phyto-group of *C. japonica*, Sichuan Camellia is a unique plant resource in Sichuan-Chongqing region of China. Characterized by its graceful form and remarkable cold tolerance, Sichuan Camellia blooms vibrantly from November to April, yet few varieties bloom in the summer and autumn. To address this limitation, we investigated three selected germplasm materials: the winter–spring flowering *C. japonica* 'Tieke Baozhu' (December–March), the summer–autumn flowering *C. azalea* (June–October), and their hybrid *Camellia* 'Lingnan Yuanbao' exhibiting paternal flowering characteristics. Through integrated transcriptomic and metabolomic analyses of these germplasms, this study aims to elucidate the molecular mechanisms underlying flowering time variation and identify key regulatory pathways for breeding Sichuan Camellia with extended flowering time.

The core mechanisms of plant flowering time regulation have been largely clarified, involving a precise set of regulatory modes. There are mainly five flowering regulatory pathways in plants, including the photoperiod pathway, the autonomous pathway, the vernalization pathway, the aging pathway, and the gibberellin (GA) pathway [7]. These pathways are integrated to regulate the expression of flowering-related genes, such as FLOWER LOCUS T (*FT*), FLOWERING LOCUS C (*FLC*), CONSTANS (*CO*), SUPPRESSOR OF HOW 1 (*SOC1*), APETALA1 (*AP1*), and LEAFY (*LFY*) [8–12]. The expression of the above key genes affecting plant flowering is mostly regulated by light or temperature, and these genes cooperate in the early stage of plant flowering, enabling plants to accurately control flowering time under specific environmental conditions [13]. Additionally, studies have compared the flowering control of plants with different life histories, showing differences in the regulatory mechanisms between annuals and perennials [14]. Research on the genetic control of flowering in perennial plants needs further refinement. More flowering-related genes have been identified and studied in plants, with some gene families showing structural and functional redundancy [15]. However, some genes exhibit different performance traits, and their functions require further exploration.

Plant hormones serve as essential endogenous regulators of flowering processes [16], with GA playing a central role through DELLA protein-mediated pathways [17–19]. Other endogenous plant hormones such as ABA [20], JA [21], auxin (AUX) [22], cytokinin (CTK) [23], salicylic acid (SA) [24], and ethylene (ET) [25] form an intricate regulatory network. While research advancements have been made in elucidating external environmental influences [26] and identifying flowering-regulatory genes [27] in *Camellia*, current studies predominantly focus on exogenous substance application for flowering time regulation [28], lacking the analysis of the molecular mechanisms underlying flowering time variations among *Camellia* germplasms. Our previous observations of contrasting flowering times between parental germplasms (*C. japonica* 'Tieke Baozhu' vs. *C. azalea*) and their hybrid

Camellia 'Lingnan Yuanbao' provide a unique opportunity to investigate these mechanisms through multi-omics integration. By combining differentially expressed genes analysis, transcription factor analysis, and integrated analysis of transcriptome and metabolome, we aim to identify critical regulators of flowering time variation, thereby advancing molecular breeding strategies for Sichuan Camellia with year-round flowering.

2. Materials and Methods

2.1. Plants and Sample Preparation

This study was conducted in 2023 at the pilot test base of the Chongqing Landscape and Gardening Research Institute, and the experimental materials were preserved by the institution (Supplementary Figure S5). During the sampling period in June, the mean daily temperature was 25–28 °C, with a photoperiod of approximately 14–14.5 h of daylight (sunrise 05:50–06:00, sunset 20:00–20:10). Relative humidity averaged 75–85%, consistent with typical early-summer conditions in Chongqing. To ensure unbiased representation, a completely randomized design (CRD) was employed for sample collection. The plant materials selected for sequencing were the buds of *C. japonica* 'Tieke Baozhu' (M), *C. azalea* (P), and their hybrid *Camellia* 'Lingnan Yuanbao' (T), with bud samples exhibiting uniform morphological characteristics (diameter: 8–10 mm; sepal closure status) in June 2023. All plants received standardized cultivation management, including daily irrigation, weekly foliar fertilization (N-P-K 20-20-20), and consistent light exposure in open-field conditions. *C. japonica* 'Tieke Baozhu' blooms from December to March of the following year, entering summer dormancy with unopened buds during June sampling. Both *C. azalea* and *Camellia* 'Lingnan Yuanbao' transition from vegetative to reproductive growth in June, initiating flowering time from June to October under long-day photoperiods and warm temperatures characteristic of Chongqing summers. At sampling time, these two germplasms were in the early floral initiation stage, showing fresh bloom characteristics. After the 1 g material was collected, it was immediately treated with liquid nitrogen and stored at −80 °C. A total of three biological replicate samples were established for transcriptomics, metabolomics, and targeted plant hormone analysis.

2.2. RNA Extraction, Library Construction, and Transcriptome Sequencing

Approximately 0.2 g of bud samples were extracted by ethanol precipitation and CTAB-pBIOZOL. Total RNA was identified and quantified using a Qubit fluorescence quantifier (Invitrogen, Carlsbad, CA, USA) and a Qsep400 high-throughput biofragment analyzer (Auto Q Biosciences, Reading, UK). Then, high-quality RNAs were selected for library construction. The mRNAs with polyA tails were enriched by oligo (dT) magnetic beads and cleaved into small fragments with fragmentation buffer at a suitable temperature. First-strand cDNAs were produced by reverse transcription using a random hexamer primer. When second-strand cDNAs were synthesized, to realize the strand-specificity, dUTPs were used instead of dTTPs in the second-strand synthesis to incorporate dUTPs, while simultaneously performing end repair and dA-tailing. Sequencing adapter ligation was performed, followed by DNA magnetic bead purification and fragment selection after ligation was completed to yield a library with 250–350 bp insert fragments. The ligated products were amplified by PCR and purified again using DNA magnetic beads. After passing the quality check, the cDNA libraries were sequenced on the Illumina sequencing platform by Metware Biotechnology Co., Ltd. (Wuhan, China).

The raw data were filtered using fastp (v0.23.2), and all subsequent analyses were based on clean reads. Transcriptome assembly of clean reads was performed using Trinity (v2.13.2), and the assembled transcripts were clustered and de-redundant using Corset (v1.09). TransDecoder (v5.3.0) was used to perform CDS prediction of Trinity-assembled

transcripts to obtain the corresponding amino acid sequences. The expression level of the transcripts was calculated using RSEM (v1.3.1), and then FPKM was calculated for each transcript based on transcript length. All transcripts were annotated by KEGG (https://www.kegg.jp/kegg, accessed on 23 August 2023), GO (https://geneontology.org, accessed on 23 August 2023), NR (https://www.ncbi.nlm.nih.gov/, accessed on 23 August 2023), and Swiss-Prot (https://www.uniprot.org/, accessed on 23 August 2023) databases using DIAMOND (v2.0.9). The principal component analysis (PCA) and K-means analysis were performed using R packages (v4.1.2). The raw data of RNA-seq were stored in NGDC (PRJCA034748).

2.3. Identification of DEGs and Enrichment Analysis

Differential expression analysis between samples was performed using DESeq2 (v1.22.2). Genes with both false discovery rate (FDR) < 0.05 and $|\log2\,(\text{ratio})| \geq 1$ were considered to be DEGs in this study. GO and KEGG enrichment analysis of DEGs (p-value ≤ 0.05) was performed based on the hypergeometric test. iTAK (http://itak.feilab.net/cgi-bin/itak/index.cgi, accessed on 23 August 2023) was used for transcription factor prediction.

2.4. Metabolite Extraction and UPLC-MS/MS Analysis

The biological samples, consisting of sepal-removed floral buds, were placed in a lyophilizer (Scientz-100F, SCIENT Z, Ningbo, China) and then ground (30 Hz, 1.5 min) to powder using a grinder (MM 400, Retsch, Haan, Germany). Next, 50 mg of sample powder was weighed and vortexed with pre-cooled 70% methanol (v/v) for 30 s, once every 30 min, for a total of 6 times. After centrifugation, the supernatant was aspirated, and the sample was filtered through a microporous membrane (0.22 μm pore size) and stored in the injection vial for UPLC-MS/MS analysis.

The sample extracts were analyzed using a UPLC-ESI-MS/MS system (UPLC, ExionLC™ AD, AB SCIEX, Framingham, MA, USA; MS, QTRAP® 6500+, AB SCIEX, Framingham, MA, USA). Based on the MetWare database, the substance qualitative analysis was performed according to the secondary spectrum information, and the metabolites were quantified by multiple reaction monitoring (MRM). Analyst (v1.6.3) was used to process and analyze mass spectrometry data, and MultiQuant (v3.0.3) was used to integrate and correct the chromatographic peaks. For two-group analysis, differential metabolites were determined by variable importance in projection (VIP) > 1 and $|\text{Log2FC}| \geq 1.0$. Identified metabolites were annotated using the KEGG compound database.

2.5. Extraction and Detection of Plant Hormones

Freshly collected sepal-removed floral buds were cryo-ground into powder, from which 50 mg of the samples was weighed and dissolved in ice-cold methanol/water/formic acid solution (15:4:1, $v/v/v$). Internal standard mixed solution (100 ng/mL) was added to the extract as internal standards (IS) for quantification. The mixture was vortexed and centrifuged, the supernatant was transferred and evaporated to dryness, then dissolved in 80% methanol (v/v), and filtered through a 0.22 μm membrane filter for further LC-MS/MS analysis. Plant hormone contents were detected by MetWare, Wuhan, China (http://www.metware.cn/, accessed on 23 August 2023) based on the AB Sciex QTRAP® 6500+ LC-MS/MS platform. Follow previous research for guidance on the operation process [29–31].

2.6. Combined Transcriptome and Metabolome Analysis

The Pearson correlation coefficient (PCC) was calculated between genes or metabolites using the cor function in R (v4.2.0). To construct the correlation network, DEGs and DAMs with $|PCC| \geq 0.8$ and p-value ≤ 0.05 were selected and illustrated using Cytoscape (v3.8).

2.7. Validation of DEGs by RT-qPCR Analysis

The expression levels of DEGs involved in multiple pathways, which showed significant differential expression in TT vs. MT, were detected by real-time fluorescence quantitative PCR (RT-qPCR). *GAPDH*, the housekeeping gene in *Camellia*, was used as the internal reference. Total RNA was treated with DNase I (Takara, Otsu, Shiga, Japan, 1 U/μg RNA, 37 °C for 30 min) prior to reverse transcription to eliminate genomic DNA contamination. The relative gene expression level was calculated using the $2^{-\Delta\Delta CT}$ method. Three biological repeats were performed. Supplementary Table S1 lists all primers used for qRT-PCR in this study.

3. Results

3.1. Screening of Differentially Expressed Genes from Transcriptome

After filtering out low-quality reads from the raw data, a total of 392,484,490 clean reads were obtained through transcriptome sequencing. The percentages of Q30 and GC were 94.58–95.64% and 44.70–45.23%, respectively (Supplementary Figure S1), indicating high-quality transcriptome sequencing data. A total of 37,848 DEGs (11,573 upregulated and 10,116 downregulated) were identified in TT vs. MT (Figure 1A), and 36,980 DEGs (8377 upregulated and 9771 downregulated) were identified in PT vs. MT (Figure 1B).

The Gene Ontology (GO) enrichment analysis was performed of DEGs in TT vs. MT and PT vs. MT. The results showed that the GO enrichment terms of the two groups were similar (Figure 1C,D), focusing on 'cellular process', 'metabolic process', 'anatomical cellular entity', 'binding', 'catalytic activity', and other pathways. The Kyoto Encyclopedia of Genes and Genomes (KEGG) enrichment analysis of DEGs in the two groups also showed similarities (Figure 1E,F), including 'Flavonoid biosynthesis', 'Phenylpropanoid biosynthesis', 'Cutin', 'suberine' and 'wax biosynthesis', 'Pentose and glucuronate interconversions', and 'Galactose metabolism'. Furthermore, in addition to the above pathways, DEGs were also significantly enriched in 'Plant hormone signal transduction' and 'ABC transporters' in PT vs. MT.

Partial DEGs exhibited the same expression pattern between TT vs. MT and PT vs. MT. The Venn diagram showed that a total of 8233 DEGs were identified in the two sets of comparisons, including 2583 upregulated and 5037 downregulated (Figure 2A). KEGG enrichment analysis revealed that these DEGs were significantly concentrated in 'Plant hormone signal transduction' (151), 'MAPK signalling pathway' (120), 'Biosynthesis of cofactors' (107), 'Phenylpropanoid biosynthesis' (96), 'Flavonoid biosynthesis' (67), 'Pyruvate metabolism' (56), 'Plant pathogen interaction' (307), and other pathways (Figure 2B). Additionally, 25 genes were differentially expressed in 'Circadian rhythm-plant', which are highly related to plant flowering induction, including 8 *PIF3*, 3 *CRY*, 3 *TOC1*, and 3 chalcone synthase (*CHS*) (Supplementary Figure S2). KEGG enrichment analysis was further performed on the co-upregulated and co-downregulated genes. Transcriptomic analysis revealed that co-upregulated genes were significantly enriched in 'Flavonoid biosynthesis' (Figure 2C), whereas co-downregulated genes were predominantly involved in 'Sesquiterpenoid and triterpenoid biosynthesis' pathways, as well as other related metabolic processes.

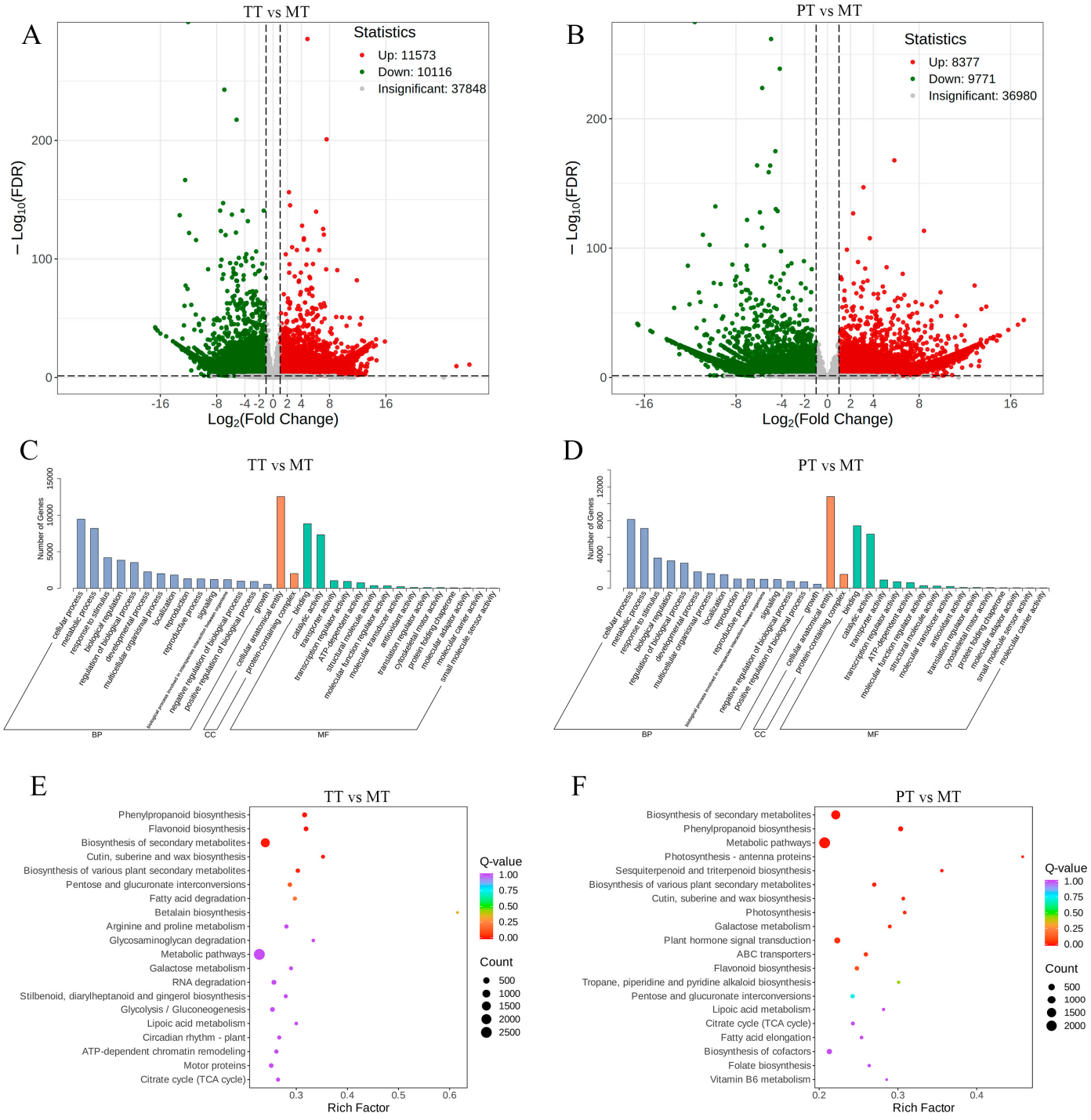


Figure 1. Screening of DEGs. (**A**) Volcano map of DEGs in TT vs. MT; (**B**) volcano map of DEGs in PT vs. MT; (**C**) GO terms of DEGs in TT vs. MT; (**D**) GO terms of DEGs in PT vs. MT; (**E**) KEGG pathway analysis of DEGs in TT vs. MT; (**F**) KEGG pathway analysis of DEGs in PT vs. MT.

3.2. Analysis of Differentially Expressed Transcription Factors

We analyzed transcription factors in TT vs. MT and PT vs. MT, and found these TFs identified belonged to 80 different families (Figure 3A,B). Analysis of TFs jointly identified in two groups revealed a total of 300 TFs that can be classified into 50 TF families (Supplementary Figure S3). These families were, in order, bHLH 9% (7 up, 20 down), MYB-related 7.67% (10 up, 13 down), MYB 5.67% (8 up, 9 down), C3H 5.67% (7 up, 10 down), B3 5% (11 up, 4 down), NAC 5% (4 up, 11 down), C2H2 4.67% (10 up, 4 down), AP2/ERF-ERF 4.33% (7 up, 6 down), bZIP 4% (6 up, 6 down), and LOB 4% (3 up, 9 down) (Figure 3C).

They all showed significant expression differences and may play an important role in the regulation of flowering time in *Camellia*.

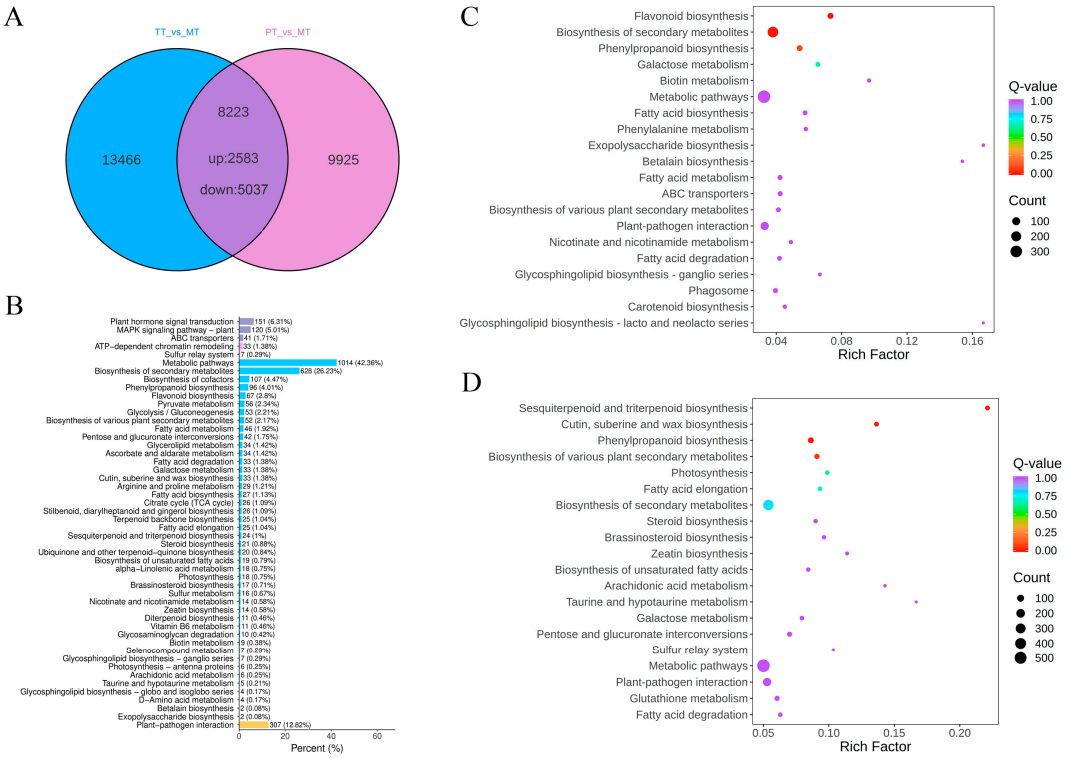


Figure 2. Co-upregulation and co-downregulation analysis of DEGs. (**A**) Venn diagram of DEGs obtained from TT vs. MT and PT vs. MT; (**B**) KEGG enrichment of DEGs obtained from TT vs. MT and PT vs. MT; (**C**) KEGG enrichment analysis of co-upregulated DEGs; (**D**) KEGG enrichment analysis of co-downregulated DEGs.

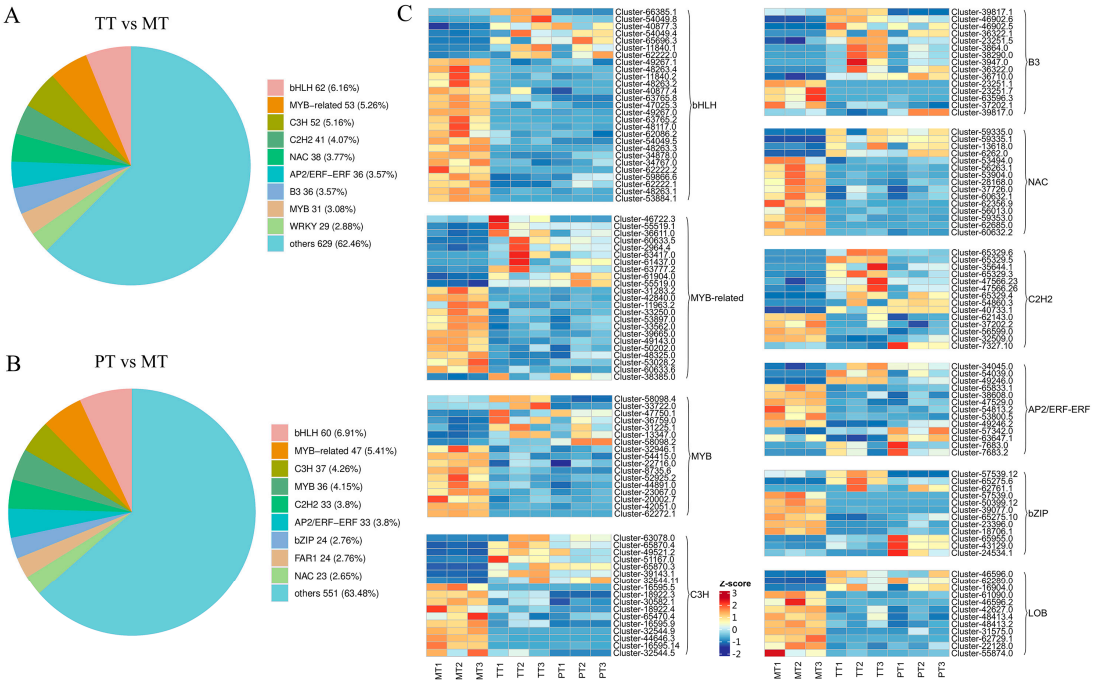


Figure 3. Annotation and classification of transcription factor. (**A**) Classification pie chart of TFs in TT vs. MT; (**B**) classification pie chart of TFs in PT vs. MT; (**C**) TF families obtained from TT vs. MT and PT vs. MT and expression analysis.

3.3. Screening of Differential Accumulated Metabolites from Metabolome

To further analyze DAMs in buds, extensive targeted metabolomics analysis was performed on TM, MM, and PM based on the UPLC-MS/MS assay platform and a self-constructed database (Supplementary Figure S1). A total of 1882 metabolites were obtained in all samples (Figure 4A), including flavonoids (25.66%), phenolic acids (16.95%), lignans and coumarins (7.49%), lipids (7.17%), terpenoids (6.85%), amino acids and derivatives (5.9%), alkaloids (5.63%), tannins (3.67%), organic acids (3.35%), nucleotides and derivatives (2.87%), quinones (0.85%), steroids (0.11%), etc. (Figure 4B).

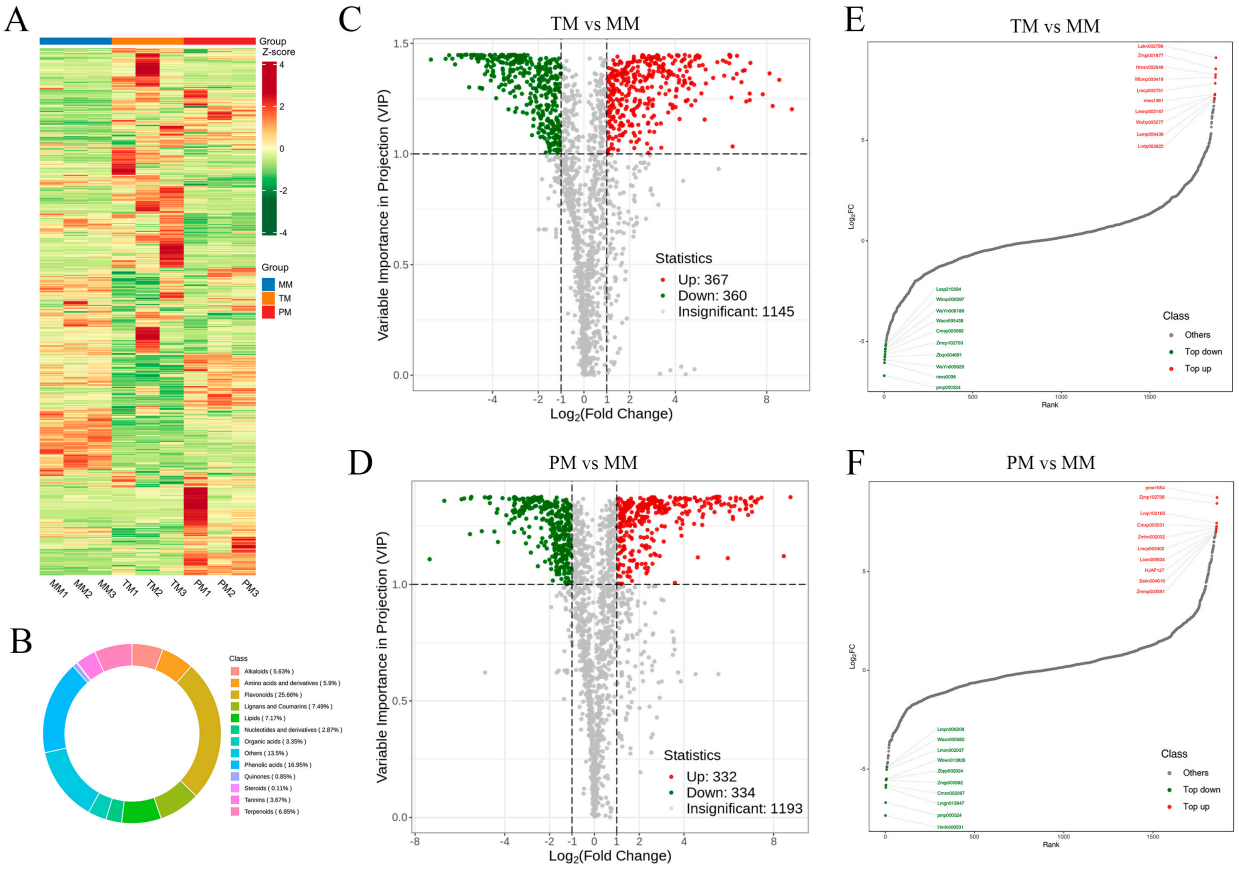


Figure 4. Screening of DAMs. (**A**) Heat map visualization of metabolites. The content of each metabolite was normalized to complete linkage hierarchical clustering. Each example is visualized in a single column, and each metabolite is represented by a single row. Red indicates high abundance and green indicates low content; (**B**) category composition of metabolites; (**C**) volcano map of DAMs in TM vs. MM; (**D**) volcano map of DAMs in PM vs. MM; (**E**) dynamic distribution of metabolite content difference in TM vs. MM. Each point represents a metabolite. Green points indicate downregulation of the top 10 metabolites, and red points indicate upregulation of the top 10 metabolites; (**F**) dynamic distribution of metabolite content difference in PM vs. MM.

Based on the OPLS-DA model, we compared and analyzed the changes of metabolites in TM and PM separately, using MM as a control, and screened for DAMs. A total of 1872 DAMs were identified in TM vs. MM (Figure 4C), of which 367 were significantly upregulated, including phenolic acids, flavonoids, terpenoids, and alkaloids (Figure 4E), and 360 were significantly downregulated, including lignans and coumarins, terpenoids, amino acid derivatives, and flavonoids. A total of 1859 DAMs were identified in PM vs. MM (Figure 4D), of which 332 were significantly upregulated, including phenolic acids, flavonoids, terpenoids, and organic acids (Figure 4F), and 334 were significantly downregulated, including lignans and coumarins, phenolic acids, terpenoids, and flavonoids.

3.4. KEGG Functional Annotation and Enrichment Analysis of DAMs

A total of 355 DAMs were identified in both the TM vs. MM and PM vs. MM groups (Figure 5A). By KEGG annotation and enrichment classification (Figure 5B), DAMs were found to be mainly enriched in 'Isorhamnetin O-glycosides biosynthesis', 'Apigenin C-glycosides biosynthesis', 'Flavone and flavonol biosynthesis', 'Biosynthesis of anthocyanins I', 'Luteolin aglycones biosynthesis', 'Biosynthesis of quercetin aglycones I' and 'Flavonoid biosynthesis' pathways.

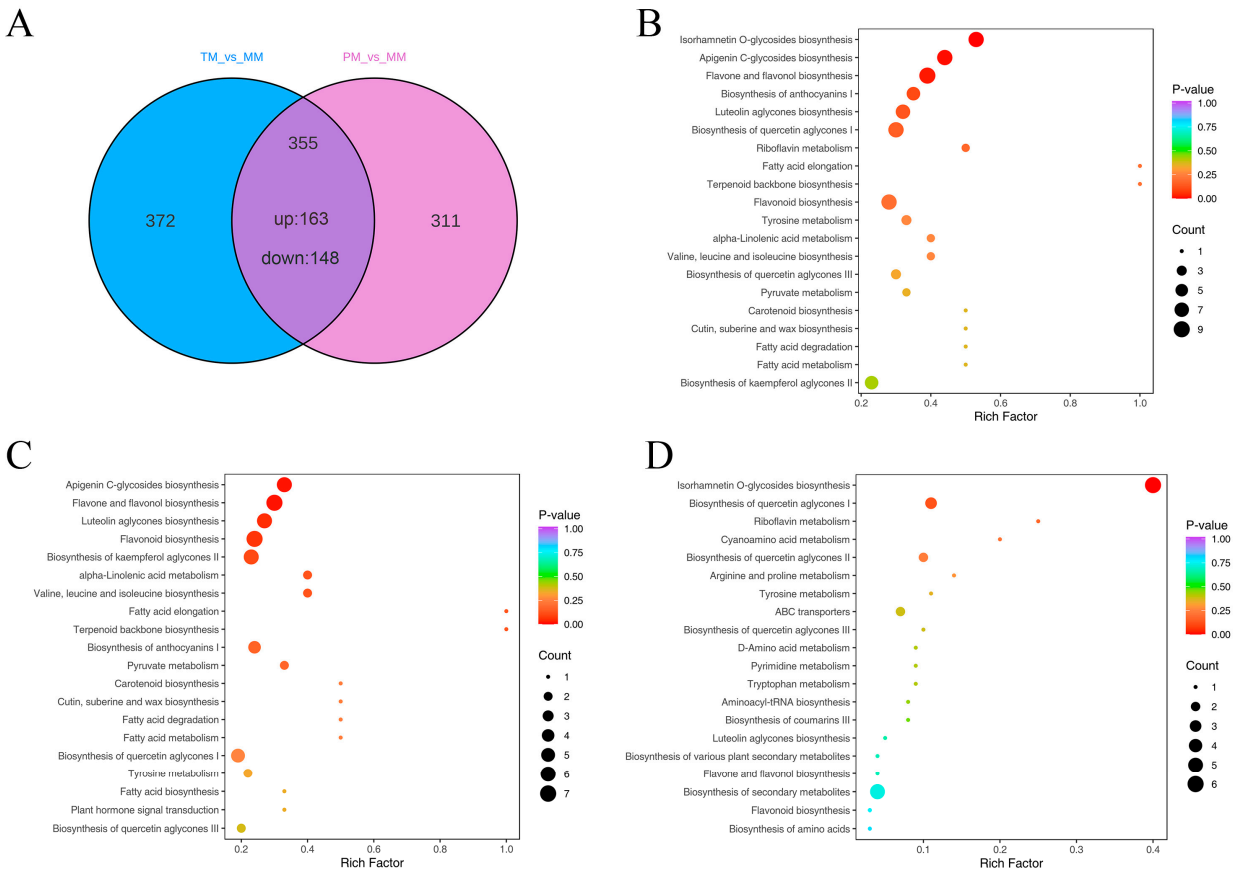


Figure 5. KEGG enrichment analysis of DAMs. (**A**) Venn diagram of DAMs obtained from TM vs. MM and PM vs. MM; (**B**) KEGG enrichment analysis of DAMs obtained from TM vs. MM and PM vs. MM; (**C**) KEGG enrichment analysis of co-upregulated DAMs; (**D**) KEGG enrichment analysis of co-downregulated DAMs.

Analysis of significantly different metabolites with the same expression pattern showed that 163 metabolites were co-upregulated (Figure 5C) and 148 metabolites were co-downregulated (Figure 5D) between TM vs. MM and PM vs. MM. Co-upregulated metabolites were mainly enriched in 'Apigenin C-glycosides biosynthesis', 'Flavone and flavonol biosynthesis', 'Luteolin aglycones biosynthesis' pathways, and the co-downregulated metabolites were mainly enriched 'Isorhamnetin O-glycosides biosynthesis', 'Biosynthesis of quercetin aglycones I' pathways.

3.5. Integrated Analysis of the Transcriptome and Metabolome

To evaluate the correlation between DEGs and DAMs, screen key genes that cause changes in metabolites and determine key regulatory pathways. The DEGs and DAMs co-enriched in the KEGG pathway were analyzed. The results showed that the pathways co-enriched by transcriptome and metabolome in both groups mainly included 'Arginine and proline metabolism', 'Tryptophan metabolism', 'Carotenoid biosynthesis', 'Phenylalanine

metabolism', 'Vitamin B6 metabolism', 'Fatty acid elongation', 'Flavonoid biosynthesis', 'Cutin, suberine and wax biosynthesis' and 'Phenypropanoid biosynthesis', and the DEGs and DAMs were significantly enriched (Figure 6A,B). Additionally, combining the pathway enrichment significance in the transcriptome and metabolome (Figure 6C,D), it was found that the genes and metabolites in the plant hormone signal transduction pathway and the flavonoid biosynthesis pathway were significantly different.

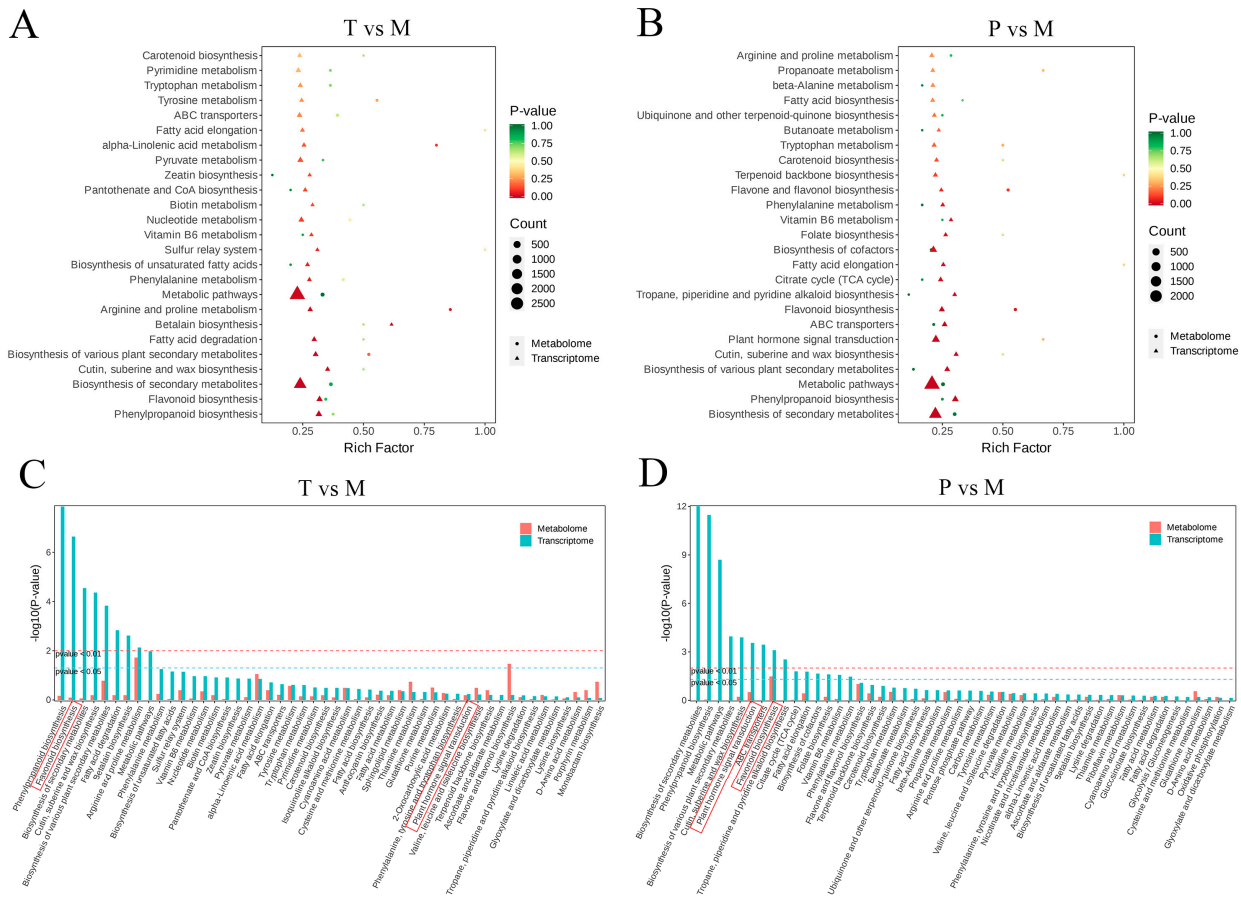


Figure 6. Integrated analysis of the transcriptomic and metabolomes. (**A**) KEGG enrichment analysis bubble plot in T vs. M; (**B**) KEGG enrichment analysis bubble plot in P vs. M; (**C**) KEGG enrichment analysis histogram in T vs. M; (**D**) KEGG enrichment analysis histogram in P vs. M. The red boxes highlight the pathways with significantly different genes and metabolites.

3.6. Analysis of Plant Hormone Signal Transduction Pathway

Based on the above-mentioned results, it is speculated that plant hormones are likely to regulate the flowering process in *Camellia* as an endogenous factor. To verify this hypothesis, nine plant hormones were quantitatively detected, and the plant hormone signal transduction pathway was further analyzed in combination with transcriptome data. The results of plant hormone content determination in all samples showed that, compared with MM, the overall plant hormone levels of TM and PM were upregulated, and the contents of GA, ABA, and JA were significantly upregulated (Figure 7). In both TT vs. MT and PT vs. MT groups, 151 DEGs associated with plant hormone signal transduction were jointly screened, of which 54 genes were co-upregulated and 82 genes were co-downregulated. There were 27 key genes (7 co-upregulated and 17 co-downregulated) associated with GA signal transduction, including 5 gibberellin-insensitive dwarf1 (*GID1*) genes (*Cluster-34690.6*, *Cluster-41765.0*, *Cluster-41765.5*, *Cluster-55591.1*, *Cluster-65584.0*) with co-downregulated expression, 5 *DELLA* genes (*Cluster-23678.0*, *Cluster-*

41686.0, *Cluster-41732.0*, *Cluster-41732.2*, *Cluster-49792.1*) with co-downregulated expression, and 7 bHLH transcription factors (*Cluster-34878.0*, *Cluster-48117.0*, *Cluster-48263.1*, *Cluster-48263.2*, *Cluster-48263.3*, *Cluster-48263.4*, *Cluster-62086.2*) with co-downregulated expression. Exactly 23 genes (6 co-upregulated and 16 co-downregulated) were related to auxin signal transduction, of which 8 auxin response factors (*ARF*) genes were co-downregulated (*Cluster-31575.0*, *Cluster-42627.0*, *Cluster-48413.2*, *Cluster-48413.4*, *Cluster-60743.9*, *Cluster-63373.4*, *Cluster-63708.6*, *Cluster-65110.2*) and 5 small auxin-up RNA (*SUAR)* genes were co-downregulated (*Cluster-30741.0*, *Cluster-38032.0*, *Cluster-39886.1*, *Cluster-53634.3*, *Cluster-56013.0*). Eleven genes (5 co-upregulated and 4 co-downregulated) were associated with ABA signal transduction, including one sucrose non-fermenting-1-related protein kinase 2 (*SnRK2*) gene downregulated (*Cluster-53616.6*) and three ABA-responsive element (ABRE) binding factor (*ABF*) genes downregulated (*Cluster-21200.0*, *Cluster-23396.0*, *Cluster-55117.3*). Eleven genes were related to JA signal transduction (four upregulated and five downregulated), of which five myelocytomatosis proteins and two (*MYC2*) genes were downregulated (*Cluster-34767.0*, *Cluster-53884.1*, *Cluster-54049.5*, *Cluster-59866.4*, *Cluster-59866.6*). The correlation analysis (Supplementary Figure S4) of the transcriptome and the targeted plant hormone metabolome showed that the above plant hormones were regulated by multiple genes, and it was speculated that these genes played different roles in hormone-mediated flowering regulation.



Figure 7. Analysis of DEGs and DAMs related to the plant hormone signal transduction pathway. The red–blue gradient of the differential metabolites in the figure represents the change of their content from high to low, and the red–green gradient of the differential genes represents the change of the expression level from high to low. The heat map abscissa sample order is M-T-P, and three biological replicates are set, respectively.

3.7. Analysis of Flavonoid Biosynthesis Pathway

In addition to plant hormones, flavonoids were also the key metabolites mined by the KEGG database, and the interaction of DEGs and DAMs related to the flavonoid biosynthesis pathway was further analyzed (Figure 8A). Compared with MM, the content of myricetin in TM and PM was lower. Apigenin-7-O-(2′-apiosyi) glucoside (Apiin)*, Apigenin-6-C-glucoside (lsovitexin)*, Apigenin-8-C-Glucoside (Vitexin)*, Quercetin-3-O-Sulfonate, Kaempferol-3-O-sophoroside, Luteolin (5,7,3′,4′-Tetrahydroxyflavone), Kaempferol-3-O-glucoside (Astragalin)*, Quercetin-3-O-rhamnoside (Quercitrin) metabolites showed higher levels (Figure 8C). The expression of five genes (*Cluster-50467.2*, *Cluster-56007.4*, *Cluster-13943.1*, *Cluster-61068.6*, *Cluster-65559.12*) related to flavonoid biosynthesis pathway was highly co-upregulated, and the expression of five genes (*Cluster-34296.1*, *Cluster-27453.0*, *Cluster-21185.6*, *Cluster-25321.0*, *Cluster-19808.8)* was co-downregulated (Figure 8B).

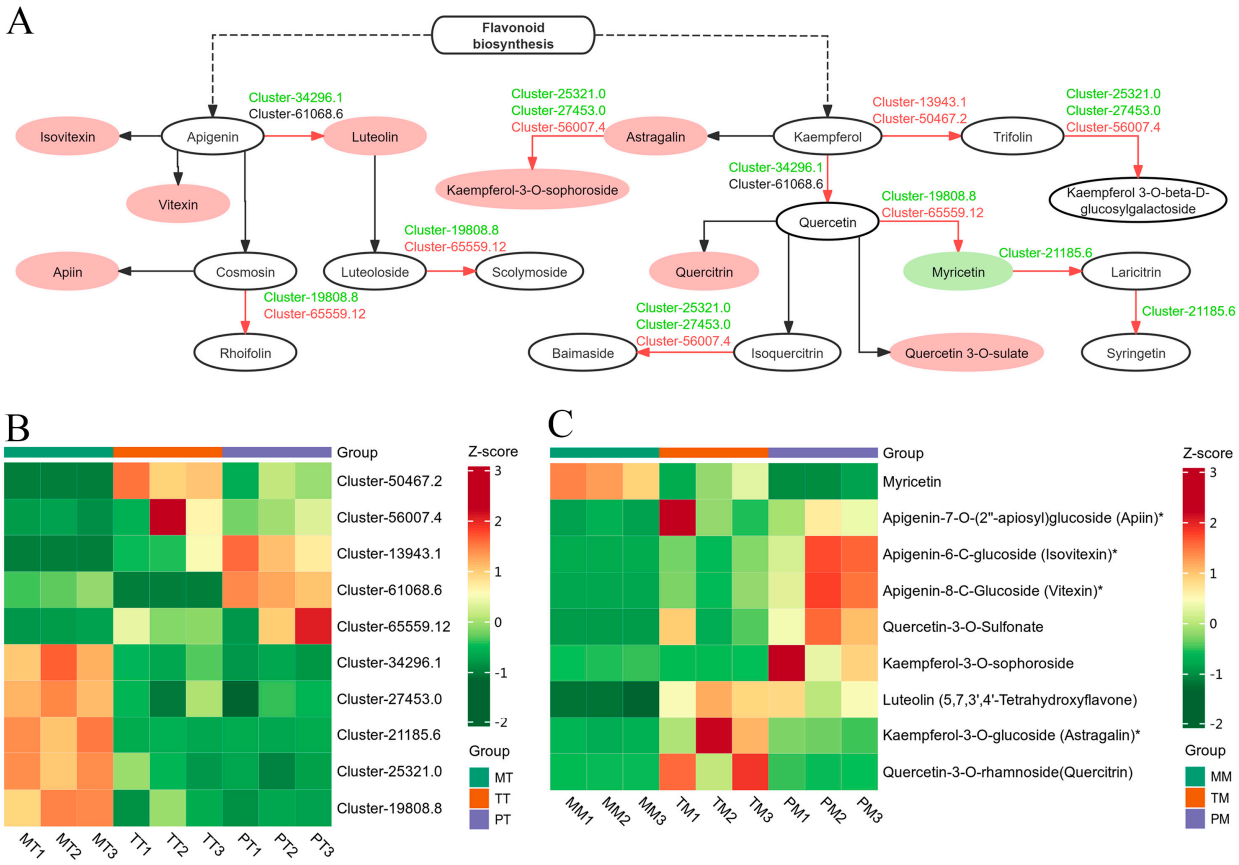


Figure 8. Analysis of DEGs and DAMs related to the flavonoid biosynthesis pathway. (**A**) The DEGs and DAMs involved in the flavonoid biosynthesis pathway. Upregulated genes and metabolites were marked in red, downregulated genes and metabolites were marked in green; (**B**) heatmap of DEGs in flavonoid biosynthesis pathway; (**C**) heatmap of DAMs in flavonoid biosynthesis pathway. Metabolites marked with an asterisk (*) indicate the presence of isomers during detection.

3.8. Expression Validation of RNA-Seq Data by RT-qPCR

To verify the reliability of the transcriptome data, 20 DEGs obtained from RNA-Seq were selected for qRT-PCR analysis. These DEGs were distributed in multiple KEGG pathways and had significantly different expression levels between TT and MT. The primer sequences used for RT-qPCR analysis are detailed in Supplementary Table S1. The Ct average values for *GAPDH* ranged between 19.7047 (TT) and 20.0176 (MT) across all samples, indicating stable expression under experimental conditions. The results showed

that the expression levels of these DEGs were consistent with the FPKM values detected by RNA-Seq (Figure 9), confirming the reliability of the analysis data from the transcriptome.



Figure 9. RT-qPCR validation of 20 DEGs.

4. Discussion

4.1. Transcriptional Regulation of Flowering Time in Camellia

Transcription factors serve as key regulators in orchestrating diverse aspects of plant growth and development, with particular importance in mediating the floral transition. In *Camellia*, we identified differential expression of bHLH, MYB, C3H, B3, NAC, and C2H2-ZFPs families (Figure 3A), aligning with known floral regulation mechanisms in model plants [32–34]. bHLH TFs showed predominant downregulation in hybrid (TT) and paternal (PT) lines compared to maternal (MT) plants, suggesting potential negative regulatory roles in flowering initiation. This contrasts with *Arabidopsis* models, where bHLH48 directly activates *FT* [32], highlighting species-specific adaptations. MYB suppression parallels observations in Prunus species, where MYB-CDC5 represses flowering through FLC activation [33]. The C2H2 zinc finger protein (C2H2-ZFPs) were upregulated, consistent with their reported involvement in photoperiodic regulation via FLC chromatin modification [34]. These findings suggest evolutionary divergence in TF regulatory networks between *Camellia* and model species. Future studies should prioritize functional validation of CsbHLH and CsMYB using genetic engineering technology to confirm their roles in flowering suppression.

4.2. Photoperiodic Regulation and Circadian Adaptations

Photoperiod is an important information source for plants to determine diurnal and seasonal changes, as well as regulating plant growth and developmental processes, including flowering time [35]. The light signaling pathway in flowering consists of photoreceptor signaling inputs, a circadian clock, and downstream genes [36]. Plants perceive and respond to light and ambient temperature using common sets of factors, such as photoreceptors and multiple light signal transduction components [37]. The photolyase-like blue-light receptors cryptochromes (CRYs) are evolutionarily conserved photoreceptors that mediate floral initiation by integrating photoperiodic and temperature signals [38]. Photoperiodic control of Camellia flowering involves conserved light signaling components (*CRY*, *TOC1*, *PIF3*), yet exhibits unique adaptations to subtropical climates. *CRY2* upregulation correlates with

early flowering in hybrids, mirroring its role in *Arabidopsis* CO stabilization [39]. TOC1-PIF3 interaction patterns differ from temperate species [40–42], potentially reflecting adaptation to Chongqing's long-day/high-temperature conditions (June photoperiod: 14.5 h; 28 °C). In this study, *Camellia* is a long-day plant intolerant of high temperature and intense light; field observations support these molecular findings: summer-flowering germplasms (*C. azalea* and hybrid) initiate flowering at daylength thresholds $\geq$ 14 h, whereas winter-flowering C. japonica enters dormancy under identical conditions. This aligns with latitudinal clines in circadian gene expression observed in model plants [39–42], suggesting conserved photoperiod adaptation mechanisms.

4.3. Hormonal Crosstalk in Floral Initiation

Plant floral initiation is governed by an integrated hormonal network that coordinates environmental cues and genetic pathways [43–45]. In this study, the results showed that the paternal and hybrid progeny exhibited the same expression pattern at the early flowering stage, with GA, ABA, JA, and IAA-related genes and metabolites showing coordinated changes during early flowering. Studying the gene expression and content changes of plant hormones can provide an important basis for explaining the response mechanism of *Camellia* to environmental changes during early flowering.

GA signaling dominates flowering regulation [17], primarily through DELLA-mediated integration with other pathways to activate reproductive development. DELLA proteins function as core negative regulators in GA signaling, restraining plant growth [46], and GA relieves the inhibitory effect of DELLA through the ubiquitin-proteasome system. GA binding to GID1 induces conformational changes [47], enhancing GA-DELLA interaction, which enables recognition by the E3 ubiquitin ligase F-box protein SLEEPY1 (SLY1), ultimately driving DELLA ubiquitination and 26S proteasomal degradation [48,49]. DELLA mutations accelerate floral initiation, whereas their accumulation delays flowering [50]. In this study, the expression levels of the five *DELLA* genes were significantly downregulated, and the total GA content was upregulated, consistent with the phenotype that the floral initiation of the paternal and the hybrid progeny was earlier than that of the maternal. Meanwhile, DELLA proteins can interact with multiple transcriptional regulators, effectively suppressing the DNA-binding capacity of transcription factors [51]. We identified seven transcription factors from the GA signaling pathway, including the *PIF3* gene, that interact with DELLA, and the expression levels of these protein-coding genes are downregulated. Therefore, we propose that the GA-DELLA module serves as a crucial regulatory hub integrating GA with other plant hormone signal transduction pathways, which may be a key determinant of flowering time regulation in *Camellia*. The finding provide actionable targets for flowering time manipulation, and exogenous GA application could potentially fine-tune DELLA dynamics to extend the ornamental period, a hypothesis warranting field validation. Additionally, DELLA proteins can also interact with jasmonate ZIM-domain (JAZ) proteins, a key inhibitor of JA signal transduction, to reduce the inhibitory function of JAZ on its key target MYC2, thus affecting JA signal transduction [52]. GA-mediated degradation of DELLA proteins exerts negative regulation on JA signaling transduction. However, the mechanism of GA-DELLA modulation in JA signal transduction requires further experimental validation.

The regulatory role of ABA in plant flowering represents a complex process, including both positive regulatory mechanisms (e.g., activation of *FT* and *SOC1* genes under long-day conditions) [20,53] and negative regulatory mechanisms (e.g., FLC gene activation and DELLA protein modulation) [54–56], with its effects potentially varying according to environmental conditions and endogenous hormonal homeostasis. In this study, we observed downregulation of 3 ARF transcription factors with increased ABA levels in buds

of summer-flowering germplasm, which was inconsistent with the known mechanism that ABA activates *SOC1* via ABF transcription factor to promote flowering under drought stress. These findings suggest multifaceted roles of ABA in *Camellia* flowering regulation, potentially operating through the photoperiodic pathway and synergistically with other plant hormones. Notably, ABA exhibits distinct response mechanisms under stress versus non-stress conditions, and the spatiotemporally specific dual regulatory networks mediated by ABA during plant flowering remain poorly understood. However, leveraging ABA plasticity enables targeted hormone interventions to optimize flowering synchrony across variable environments.

4.4. Flavonoid Dynamics and Bud Development

Flavonoids, a kind of polyphenolic compounds with known antioxidant activity, the main categories, including flavones, flavonols, flavanones, isoflavones, anthocyanins. Flavonoid content is closely related to plant species and stage of growth and development, exhibiting significant differences between plant organs, predominantly accumulating in leaves and flowers, and their content commonly first increases and then decreases with the process of plant growth and senescence [57]. For instance, total flavonoid content in flax demonstrates initial increases followed by decreases throughout seed germination, vegetative growth, flowering, and maturation, peaking during the flowering stage [58]. In *Juglans regia*, the flavonoid content (catechin, myricetin) in the annual branches shows progressive accumulation from spring to summer [59]. Flavonoids in *Zingiber mioga* are closely related to the color formation of buds, and most metabolites tended to accumulate and reached the maximum at the maturity stage [60]. The biosynthesis of flavonoids involves complex metabolic pathways regulated by key enzymes, including CHS, chalcone isomerase (CHI), flavonol synthetase (FLS), and transcription factors (e.g., MYB, bHLH) [61,62]. Our findings reveal elevated flavonoid levels in buds of *C. azalea* and *Camellia* 'Lingnan Yuanbao' during pre-flowering stages, consistent with previous reports. Upon the onset of the flowering stage in *Camellia*, key genes encoding flavonoid biosynthetic enzymes and transcription factors are activated, promoting flavonoid biosynthesis. Thus, in *Camellia* species, flavonoid dynamics are tightly linked to phenological transitions, and bud dormancy release coincides with flavonoid accumulation, suggesting these metabolites serve as biochemical markers of bud developmental progression. Activation of flavonoid biosynthetic genes during floral initiation further supports their functional importance in *Camellia* flowering regulation.

4.5. Future Directions and Breeding Applications

The findings of this study lay a foundation for both theoretical advances and practical applications in Camellia improvement. Building on the identified photoperiod-responsive genes (e.g., CRY2) and hormone crosstalk dynamics, molecular breeding strategies could prioritize pyramiding alleles conferring photoperiod insensitivity with those enhancing GA signaling, potentially enabling the development of everblooming cultivars adapted to diverse climates. CRISPR-based editing of key genes emerges as a promising approach to decouple JA-mediated stress tolerance from flowering delay. However, critical knowledge gaps must be addressed to fully harness these opportunities, including the spatial regulation of hormone transport (e.g., GA flux from mature leaves to buds), epigenetic control of FLC homologs in *Camellia*, and cross-species applicability of flavonoid-based dormancy markers. Systematic investigation of these aspects will not only refine our understanding of flowering regulation in woody ornamentals but also accelerate the translation of omics discoveries into field-based breeding pipelines.

5. Conclusions

In this study, the transcriptome and metabolome sequencing of *C. japonica* 'Tieke Baozhu', *C. azalea*, and their hybrid *Camellia* 'Lingnan Yuanbao' were carried out to reveal the key molecular mechanisms of flowering time regulation in *Camellia*. The results showed that DEGs and DAMs were mainly enriched in the pathways related to plant hormone synthesis and signal transduction, photoperiod regulation, and flavonoid synthesis. The differential expression of bHLH and MYB transcription factor families indicated that they may regulate the flowering time of *Camellia* through plant hormone signal transduction and the photoperiod pathway. The differential expression of photoperiod-related genes *CRY*, *TOC1*, and *PIF3* further supported the key role of the photoperiod pathway. Plant hormone analysis showed that the levels of GA, ABA, and JA were significantly different among *Camellia* germplasms, and the differential expression of DELLA proteins revealed the core position of the GA signal transduction pathway. Additionally, the significant difference in flavonoid metabolite content was closely related to the developmental stage of the buds. This study provided an important theoretical basis for an in-depth understanding of the flowering time regulation mechanism in *Camellia*, and also laid a molecular foundation for the breeding and cultivation practice of *Camellia*.

Supplementary Materials: The following supporting information can be downloaded at: https://www.mdpi.com/article/10.3390/agronomy15061288/s1, Table S1: Primer sequences used for qRT-PCR; Figure S1: Transcriptome and metabolome data quality control; Figure S2: Analysis of DEGs related to plant circadian rhythm pathway; Figure S3: Classification pie chart of TFs in TT vs. MT and PT vs. MT; Figure S4: The correlation analysis of the transcriptome and the targeted plant hormones; Figure S5: *Camellia* germplasms sampled for sequencing analysis.

Author Contributions: Conceptualization, T.G. and L.Z.; data curation, L.Z.; formal analysis, L.Z. and T.G.; investigation, S.Z. and L.L.; methodology, L.A.; validation, X.L., J.W. and Z.Z.; writing—original draft, L.Z.; writing—review and editing, T.G. and L.A. All authors have read and agreed to the published version of the manuscript.

Funding: This research was funded by the Natural Science Foundation of Chongqing, China (CSTB2022NSCQ-BHX0744); Incentive and Guidance Special Project of Scientific Research Institution, Chongqing Science and Technology Committee (cstc2022jxjl80022); Chongqing Key Laboratory of Germplasm Innovation and Utilization of Native Plants (XTZW2023-ZS01).

Data Availability Statement: The data have been deposited in the National Geophysical Data Center (NGDC) under accession number PRJCA034748.

Conflicts of Interest: The authors declare no conflicts of interest.

References

1. Vijayan, K.; Zhang, W.-J.; Tsou, C.-H. Molecular taxonomy of *Camellia* (Theaceae) inferred from nrITS sequences. *Am. J. Bot.* **2009**, *96*, 1348–1360. [CrossRef] [PubMed]
2. Kim, S.-H.; Hyun, C.C.; Misuk, Y.; Kim, S.-C. The complete chloroplast genome sequence of the Japanese Camellia (*Camellia japonica* L.). *Mitochondrial DNA Part B* **2017**, *2*, 583–584. [CrossRef]
3. Vela, P.; Salinero, C.; Sainz, M.J. Phenological growth stages of *Camellia japonica*. *Ann. Appl. Biol.* **2013**, *162*, 182–190. [CrossRef]
4. Wang, Y.; Zhuang, H.; Shen, Y.; Wang, Y.; Wang, Z. The Dataset of *Camellia* Cultivars Names in the World. *Biodivers. Data J.* **2021**, *9*, 61646. [CrossRef]
5. Ren, H.; Jian, S.; Chen, Y.; Liu, H.; Zhang, Q.; Liu, N.; Xu, Y.; Luo, J. Distribution, status, and conservation of *Camellia changii* Ye (Theaceae), a Critically Endangered plant endemic to southern China. *Oryx* **2014**, *48*, 358–360. [CrossRef]
6. Fan, Z.; Li, J.; Li, X.; Wu, B.; Wang, J.; Liu, Z.; Yin, H. Genome-wide transcriptome profiling provides insights into floral bud development of summer-flowering *Camellia azale*. *Sci. Rep.* **2015**, *5*, 9729. [CrossRef]
7. Niu, F.; Rehmani, M.S.; Yan, J. Multilayered regulation and implication of flowering time in plants. *Plant Physiol. Biochem.* **2024**, *213*, 108842. [CrossRef] [PubMed]

8. Corbesier, L.; Vincent, C.; Jang, S.; Fornara, F.; Fan, Q.; Searle, I.; Giakountis, A.; Farrona, S.; Gissot, L.; Turnbull, C.; et al. FT protein movement contributes to long-distance signaling in floral induction of *Arabidopsis*. *Science* **2007**, *316*, 1030–1033. [CrossRef] [PubMed]
9. Tiwari, S.B.; Shen, Y.; Chang, H.C.; Hou, Y.; Harris, A.; Ma, S.F.; McPartland, M.; Hymus, G.J.; Adam, L.; Marion, C.; et al. The flowering time regulator CONSTANS is recruited to the FLOWERING LOCUS T promoter via a unique cis-element. *New Phytol.* **2010**, *187*, 57–66. [CrossRef]
10. Sharma, N.; Geuten, K.; Giri, B.S.; Varma, A. The molecular mechanism of vernalization in *Arabidopsis* and cereals: Role of Flowering Locus C and its homologs. *Physiol. Plant* **2020**, *170*, 373–383. [CrossRef]
11. Sharma, N.; Ruelens, P.; D'hauw, M.; Maggen, T.; Dochy, N.; Torfs, S.; Kaufmann, K.; Rohde, A.; Geuten, K. A Flowering Locus C Homolog Is a Vernalization-Regulated Repressor in Brachypodium and Is Cold Regulated in Wheat. *Plant Physiol.* **2016**, *173*, 1301–1315. [CrossRef]
12. Ferrándiz, C.; Gu, Q.; Martienssen, R.; Yanofsky, M.F. Redundant regulation of meristem identity and plant architecture by FRUITFULL, APETALA1 and CAULIFLOWER. *Development* **2000**, *127*, 725–734. [CrossRef] [PubMed]
13. Andrés, F.; Coupland, G. The genetic basis of flowering responses to seasonal cues. *Nat. Rev. Genet.* **2012**, *13*, 627–639. [CrossRef]
14. Rehman, S.; Bahadur, S.; Xia, W. An overview of floral regulatory genes in annual and perennial plants. *Gene* **2023**, *885*, 147699. [CrossRef]
15. Davière, J.-M.; Achard, P. Gibberellin signaling in plants. *Development* **2013**, *140*, 1147–1151. [CrossRef] [PubMed]
16. Santner, A.; Estelle, M. Recent advances and emerging trends in plant hormone signalling. *Nature* **2009**, *459*, 1071–1078. [CrossRef] [PubMed]
17. Conti, L. Hormonal control of the floral transition: Can one catch them all? *Dev. Biol.* **2017**, *430*, 288–301. [CrossRef]
18. Bao, S.; Hua, C.; Shen, L.; Yu, H. New insights into gibberellin signaling in regulating flowering in *Arabidopsis*. *J. Integr. Plant Biol.* **2020**, *62*, 118–131. [CrossRef]
19. Zhang, C.; Jian, M.; Li, W.; Yao, X.; Tan, C.; Qian, Q.; Hu, Y.; Liu, X.; Hou, X. Gibberellin signaling modulates flowering via the DELLA-BRAHMA-NF-YC module in Arabidopsis. *Plant Cell* **2023**, *35*, 3470–3484. [CrossRef]
20. Riboni, M.; Robustelli Test, A.; Galbiati, M.; Tonelli, C.; Conti, L. ABA-dependent control of GIGANTEA signalling enables drought escape via up-regulation of FLOWERING LOCUS T in *Arabidopsis thaliana*. *J. Exp. Bot.* **2016**, *67*, 6309–6322. [CrossRef]
21. Zhai, Q.; Zhang, X.; Wu, F.; Feng, H.; Deng, L.; Xu, L.; Zhang, M.; Wang, Q.; Li, C. Transcriptional Mechanism of Jasmonate Receptor COI1-Mediated Delay of Flowering Time in *Arabidopsis*. *Plant Cell* **2015**, *27*, 2814–2828. [CrossRef] [PubMed]
22. Dong, X.; Li, Y.; Guan, Y.; Wang, S.; Luo, H.; Li, X.; Li, H.; Zhang, Z. Auxin-induced AUXIN RESPONSE FACTOR4 activates APETALA1 and FRUITFULL to promote flowering in woodland strawberry. *Hortic. Res.* **2021**, *8*, 115. [CrossRef]
23. D'Aloia, M.; Bonhomme, D.; Bouché, F.; Tamseddak, K.; Ormenese, S.; Torti, S.; Coupland, G.; Périlleux, C. Cytokinin promotes flowering of Arabidopsis via transcriptional activation of the FT paralogue TSF. *Plant J.* **2011**, *65*, 972–979. [CrossRef] [PubMed]
24. Segarra, S.; Mir, R.; Martínez, C.; León, J. Genome-wide analyses of the transcriptomes of salicylic acid-deficient versus wild-type plants uncover Pathogen and Circadian Controlled 1 (PCC1) as a regulator of flowering time in *Arabidopsis*. *Plant Cell Environ.* **2010**, *33*, 11–22. [CrossRef]
25. Achard, P.; Baghour, M.; Chapple, A.; Hedden, P.; Van Der Straeten, D.; Genschik, P.; Moritz, T.; Harberd, N.P. The plant stress hormone ethylene controls floral transition via DELLA-dependent regulation of floral meristem-identity genes. *Proc. Natl. Acad. Sci. USA* **2007**, *104*, 6484–6489. [CrossRef]
26. Lee, Z.; Kim, S.; Choi, S.J.; Joung, E.; Kwon, M.; Park, H.J.; Shim, J.S. Regulation of Flowering Time by Environmental Factors in Plants. *Plants* **2023**, *12*, 3680. [CrossRef] [PubMed]
27. Hu, Z.; Fan, Z.; Li, S.; Wang, M.; Huang, M.; Ma, X.; Liu, W.; Wang, Y.; Yu, Y.; Li, Y.; et al. Genomics insights into flowering and floral pattern formation: Regional duplication and seasonal pattern of gene expression in *Camellia*. *BMC Biol.* **2024**, *22*, 50. [CrossRef]
28. Lin, M.; Wang, S.; Liu, Y.; Li, J.; Zhong, H.; Zou, F.; Yuan, D. Hydrogen cyanamide enhances flowering time in tea oil camellia (*Camellia oleifera* Abel.). *Ind. Crops Prod.* **2022**, *176*, 114313. [CrossRef]
29. Pan, X.; Welti, R.; Wang, X. Quantitative analysis of major plant hormones in crude plant extracts by high-performance liquid chromatography-mass spectrometry. *Nat. Protoc.* **2010**, *5*, 986–992. [CrossRef]
30. Šimura, J.; Antoniadi, I.; Široká, J.; Tarkowská, D.; Strnad, M.; Ljung, K.; Novák, O. Plant Hormonomics: Multiple Phytohormone Profiling by Targeted Metabolomics. *Plant Physiol.* **2018**, *177*, 476–489. [CrossRef]
31. Cui, K.; Lin, Y.; Zhou, X.; Li, S.; Liu, H.; Zeng, F.; Zhu, F.; Ouyang, G.; Zeng, Z. Comparison of sample pretreatment methods for the determination of multiple phytohormones in plant samples by liquid chromatography–electrospray ionization-tandem mass spectrometry. *Microchem. J.* **2015**, *121*, 25–31. [CrossRef]
32. Li, Y.; Wang, H.; Li, X.; Liang, G.; Yu, D. Two DELLA-interacting proteins bHLH48 and bHLH60 regulate flowering under long-day conditions in *Arabidopsis thaliana*. *J. Exp. Bot.* **2017**, *68*, 2757–2767. [CrossRef] [PubMed]

33. Xin, X.; Ye, L.; Zhai, T.; Wang, S.; Pan, Y.; Qu, K.; Gu, M.; Wang, Y.; Zhang, J.; Li, X.; et al. CELL DIVISION CYCLE 5 controls floral transition by regulating flowering gene transcription and splicing in *Arabidopsis*. *Plant Physiol.* **2024**, *197*, 616. [CrossRef] [PubMed]
34. Lyu, T.; Cao, J. Cys2/His2 Zinc-Finger Proteins in Transcriptional Regulation of Flower Development. *Int. J. Mol. Sci.* **2018**, *19*, 2589. [CrossRef]
35. Casal, J.J.; Qüesta, J.I. Light and temperature cues: Multitasking receptors and transcriptional integrators. *New Phytol.* **2018**, *217*, 1029–1034. [CrossRef]
36. Shim, J.S.; Kubota, A.; Imaizumi, T. Circadian Clock and Photoperiodic Flowering in *Arabidopsis*: CONSTANS Is a Hub for Signal Integration. *Plant Physiol.* **2017**, *173*, 5–15. [CrossRef]
37. Li, X.; Liang, T.; Liu, H. How plants coordinate their development in response to light and temperature signals. *Plant Cell* **2021**, *34*, 955–966. [CrossRef]
38. Zhao, Z.; Dent, C.; Liang, H.; Lv, J.; Shang, G.; Liu, Y.; Feng, F.; Wang, F.; Pang, J.; Li, X.; et al. CRY2 interacts with CIS1 to regulate thermosensory flowering via FLM alternative splicing. *Nat. Commun.* **2022**, *13*, 7045. [CrossRef]
39. Guo, H.; Yang, H.; Mockler, T.C.; Lin, C. Regulation of Flowering Time by *Arabidopsis* Photoreceptors. *Science* **1998**, *279*, 1360–1363. [CrossRef]
40. Soy, J.; Leivar, P.; González-Schain, N.; Martín, G.; Diaz, C.; Sentandreu, M.; Al-Sady, B.; Quail, P.H.; Monte, E. Molecular convergence of clock and photosensory pathways through PIF3–TOC1 interaction and co-occupancy of target promoters. *Proc. Natl. Acad. Sci. USA* **2016**, *113*, 4870–4875. [CrossRef]
41. Nakamichi, N.; Kita, M.; Niinuma, K.; Ito, S.; Yamashino, T.; Mizoguchi, T.; Mizuno, T. *Arabidopsis* Clock-Associated Pseudo-Response Regulators PRR9, PRR7 and PRR5 Coordinately and Positively Regulate Flowering Time Through the Canonical CONSTANS-Dependent Photoperiodic Pathway. *Plant Cell Physiol.* **2007**, *48*, 822–832. [CrossRef] [PubMed]
42. Li, K.; Yu, R.; Fan, L.-M.; Wei, N.; Chen, H.; Deng, X.W. DELLA-mediated PIF degradation contributes to coordination of light and gibberellin signalling in *Arabidopsis*. *Nat. Commun.* **2016**, *7*, 11868. [CrossRef]
43. Li, X.; Lin, C.; Lan, C.; Tao, Z. Genetic and epigenetic basis of phytohormonal control of floral transition in plants. *J. Exp. Bot.* **2024**, *75*, 4180–4194. [CrossRef] [PubMed]
44. Campos-Rivero, G.; Osorio-Montalvo, P.; Sánchez-Borges, R.; Us-Camas, R.; Duarte-Aké, F.; De-la-Peña, C. Plant hormone signaling in flowering: An epigenetic point of view. *J. Plant Physiol.* **2017**, *214*, 16–27. [CrossRef] [PubMed]
45. Santner, A.; Calderon-Villalobos, L.I.A.; Estelle, M. Plant hormones are versatile chemical regulators of plant growth. *Nat. Chem. Biol.* **2009**, *5*, 301–307. [CrossRef]
46. Harberd, N.P. Relieving DELLA Restraint. *Science* **2003**, *299*, 1853–1854. [CrossRef]
47. Hirano, K.; Asano, K.; Tsuji, H.; Kawamura, M.; Mori, H.; Kitano, H.; Ueguchi-Tanaka, M.; Matsuoka, M. Characterization of the Molecular Mechanism Underlying Gibberellin Perception Complex Formation in Rice. *Plant Cell* **2010**, *22*, 2680–2696. [CrossRef]
48. Dill, A.; Thomas, S.G.; Hu, J.; Steber, C.M.; Sun, T.-P. The *Arabidopsis* F-Box Protein SLEEPY1 Targets Gibberellin Signaling Repressors for Gibberellin-Induced Degradation. *Plant Cell* **2004**, *16*, 1392–1405. [CrossRef]
49. Silverstone, A.L.; Ciampaglio, C.N.; Sun, T.-P. The Arabidopsis RGA Gene Encodes a Transcriptional Regulator Repressing the Gibberellin Signal Transduction Pathway. *Plant Cell* **1998**, *10*, 155–169. [CrossRef]
50. Cheng, H.; Qin, L.; Lee, S.; Fu, X.; Richards, D.E.; Cao, D.; Luo, D.; Harberd, N.P.; Peng, J. Gibberellin regulates *Arabidopsis* floral development via suppression of DELLA protein function. *Development* **2004**, *131*, 1055–1064. [CrossRef]
51. Davière, J.-M.; Achard, P. A Pivotal Role of DELLAs in Regulating Multiple Hormone Signals. *Mol. Plant* **2016**, *9*, 10–20. [CrossRef]
52. Hou, X.; Lee, L.Y.C.; Xia, K.; Yan, Y.; Yu, H. DELLAs Modulate Jasmonate Signaling via Competitive Binding to JAZs. *Dev. Cell* **2010**, *19*, 884–894. [CrossRef]
53. Riboni, M.; Galbiati, M.; Tonelli, C.; Conti, L. GIGANTEA Enables Drought Escape Response via Abscisic Acid-Dependent Activation of the Florigens and SUPPRESSOR OF OVEREXPRESSION OF CONSTANS1. *Plant Physiol.* **2013**, *162*, 1706–1719. [CrossRef]
54. Shu, K.; Chen, Q.; Wu, Y.; Liu, R.; Zhang, H.; Wang, S.; Tang, S.; Yang, W.; Xie, Q. ABSCISIC ACID-INSENSITIVE 4 negatively regulates flowering through directly promoting *Arabidopsis* FLOWERING LOCUS C transcription. *J. Exp. Bot.* **2015**, *67*, 195–205. [CrossRef] [PubMed]
55. Wang, Y.; Li, L.; Ye, T.; Lu, Y.; Chen, X.; Wu, Y. The inhibitory effect of ABA on floral transition is mediated by ABI5 in *Arabidopsis*. *J. Exp. Bot.* **2013**, *64*, 675–684. [CrossRef]
56. Achard, P.; Cheng, H.; De Grauwe, L.; Decat, J.; Schoutteten, H.; Moritz, T.; Van Der Straeten, D.; Peng, J.; Harberd, N.P. Integration of Plant Responses to Environmentally Activated Phytohormonal Signals. *Science* **2006**, *311*, 91–94. [CrossRef] [PubMed]
57. Ma, D.; Guo, Y.; Ali, I.; Lin, J.; Xu, Y.; Yang, M. Accumulation characteristics of plant flavonoids and effects of cultivation measures on their biosynthesis: A review. *Plant Physiol. Biochem.* **2024**, *215*, 108960. [CrossRef] [PubMed]
58. Zuk, M.; Szperlik, J.; Hnitecka, A.; Szopa, J. Temporal biosynthesis of flavone constituents in flax growth stages. *Plant Physiol. Biochem.* **2019**, *142*, 234–245. [CrossRef]

59. Solar, A.; Colarič, M.; Usenik, V.; Stampar, F. Seasonal variations of selected flavonoids, phenolic acids and quinones in annual shoots of common walnut (*Juglans regia* L.). *Plant Sci.* **2006**, *170*, 453–461. [CrossRef]
60. Liu, H.; Cheng, Z.; Luo, M.; Xie, J. The dynamic variations of flavonoid metabolites in flower buds for *Zingiber mioga* at different developmental stages. *J. Food Compos. Anal.* **2023**, *123*, 105537. [CrossRef]
61. Shen, N.; Wang, T.; Gan, Q.; Liu, S.; Wang, L.; Jin, B. Plant flavonoids: Classification, distribution, biosynthesis, and antioxidant activity. *Food Chem.* **2022**, *383*, 132531. [CrossRef] [PubMed]
62. Gao, Y.; Liu, J.; Chen, Y.; Tang, H.; Wang, Y.; He, Y.; Ou, Y.; Sun, X.; Wang, S.; Yao, Y. Tomato SlAN11 regulates flavonoid biosynthesis and seed dormancy by interaction with bHLH proteins but not with MYB proteins. *Hortic. Res.* **2018**, *5*, 27. [CrossRef] [PubMed]

Disclaimer/Publisher's Note: The statements, opinions and data contained in all publications are solely those of the individual author(s) and contributor(s) and not of MDPI and/or the editor(s). MDPI and/or the editor(s) disclaim responsibility for any injury to people or property resulting from any ideas, methods, instructions or products referred to in the content.